Battery Cell Identification and SOC Estimation Using String Terminal Voltage Measurements

Le Yi Wang, *Fellow, IEEE*, Michael P. Polis, *Life Senior Member, IEEE*, G. George Yin, *Fellow, IEEE*, Wen Chen, *Member, IEEE*, Yuhong Fu, and Chunting Chris Mi, *Fellow, IEEE*

***Abstract*—A battery system consists of many battery cells or modules that may have different characteristics. To achieve reliable, efficient, and extended utilization of battery systems, the battery management system (BMS) must keep track of individual cell-level dynamics, state of charge (SOC), state of health (SOH), failure status, and life-expectancy prediction. Current battery technology employs cell- or module-level voltage sensors, with high costs for sensors and packaging, and substantial reliability issues. This paper introduces new methods that utilize existing cell-balancing circuits to estimate an individual cell's voltage and current from battery string terminal voltage/current measurements. This is achieved by actively controlling balancing circuits to create partial observability for battery cell subsystems. Control strategies, estimation algorithms, and their key properties are developed. Some typical battery model structures are used to illustrate the usage of the methods.**

***Index Terms*—Balancing circuit, battery management systems (BMSs), battery systems, observability, state estimation, system identification.**

I. Introduction

BATTERY systems and their management are essential for electric vehicles (including hybrid electric, plug-in hybrid, fuel cell, and solar vehicles), renewable-energy generators, and smart grid development [1]. Battery systems consist of many battery cells or modules that could have different characteristics. Issues, such as cell aging, imbalance in thermal distributions and charge/discharge rates, and variations in chemical properties, become more pronounced during battery operation. To achieve reliable, efficient, and extended utilization of battery systems, the battery management system (BMS) must keep track of individual cell-level dynamics, state of charge (SOC), state of health (SOH), failure status, and life-expectancy prediction [2]–[6]. To accomplish this, existing approaches require individual cell's voltage and current data for internal state estimation and system identification [7]–[9], with high costs for sensors and packaging, and substantial reliability issues.

Cell balancing is an essential BMS function, particularly for Li-ion batteries [10], [11]. To supply required voltages, battery cells must be connected in series. During charge and discharge, each cell in the string will be subject to the same current but will have different SOCs due to several factors. First, cells have different maximum capacities. Even if the manufacturer makes the best effort to match capacities for new cells, nonuniform operating conditions impose different thermal and electrical stress on cells, causing changes in capacities. Second, although Li-ion cells have small self-discharge rates, small differences can accumulate over time, causing different SOCs even for cells with nearly identical capacities. Third, variations in internal impedance and material aging inevitably lead to nonuniform cell characteristics. To protect the cells from overheat, overcharge, and overdischarge, the operation of the string is fundamentally limited by the weakest cell, the one reaching SOC upper or lower boundaries first. Cell SOC imbalance in a string prevents cells from supplying their capacities fully, and consequently limits the battery run time, SOH, and life cycles. Cell balancing aims to reduce SOC imbalances within a string by controlling the SOCs of the cells so that they become approximately equal. This can be achieved by dissipating energy from the cells of higher SOCs to shunt resistors or shuffling energy from the highest SOC cell to the lowest SOC cell or by incremental cell balancing through paired cells in stages [1], [11], [12].

Battery modules are comprised of multiple strings of cells. In a conventional string setup, the voltages of each cell and the string need to be measured by voltage transducers. In addition, each string requires a string current sensor. Sensor failures reduce battery reliability. Extensive sensor deployments increase costs, packaging difficulty, and control and thermal management complexity. A technical question arises: Is it possible to derive and estimate cell internal states by using only the string terminal voltage and current data? In principle, this cannot be achieved since the system is not observable. In other words, there are always infinitely many possible internal voltage/current values that will produce the same terminal voltage.

This paper introduces new methods that utilize the existing cell-balancing circuits to estimate individual cells' voltages

Manuscript received December 21, 2011; revised March 26, 2012; accepted May 28, 2012. Date of publication June 6, 2012; date of current version September 11, 2012. This work was supported in part by the National Science Foundation under Grant ECCS-1202133. The review of this paper was coordinated by Mr. D. Diallo.

L. Y. Wang is with the Department of Electrical and Computer Engineering, Wayne State University, Detroit, MI 48202 USA (e-mail: lywang@wayne.edu).

M. P. Polis is with the Department of Industrial and Systems Engineering, Oakland University, Rochester, MI 48309 USA (e-mail: polis@oakland.edu).

G. G. Yin is with the Department of Mathematics, Wayne State University, Detroit, MI 48202 USA (e-mail: gyin@math.wayne.edu).

W. Chen is with the Division of Engineering Technology, Wayne State University, Detroit, MI 48202 USA (e-mail: wchenc@wayne.edu).

Y. Fu and C. C. Mi are with the Department of Electrical and Computer Engineering, University of Michigan-Dearborn, Dearborn, MI 48128 USA (e-mail: fuyuhong@gmail.com; chrismi@umich.edu).

Color versions of one or more of the figures in this paper are available online at http://ieeexplore.ieee.org.

Digital Object Identifier 10.1109/TVT.2012.2203160

and currents from the battery string terminal voltage–current measurements. Balancing circuits are mandatory in battery management and integrated in battery packs. Utilizing this existing hardware feature, we can achieve internal observability without detrimental effects on normal balancing operations. Using the methods of this paper removes the cost of the voltage sensors at each cell. It should be emphasized that, under any fixed balancing circuit condition, the battery system remains unobservable. However, switching of cell-balancing circuits creates a partially observable system under which some cell's voltage and current become observable from the terminal voltage/current data. By strategically controlling the balancing circuits in certain sequences, all cells become observable over time. Control strategies, estimation algorithms, and their key properties for our methodology are developed.

Many battery models have been proposed, with similar structures but different expressions or nonlinearities [13]–[18]. For concreteness in algorithm development, a typical circuit model of lithium ion batteries [10], [19], [20] and a typical nonlinear model from the SimPower Systems Toolbox in Matlab/Simulink [21], [22] are used to illustrate the methods, although such selections are not limiting factors for the methods.

In addition, this paper derives a scheme to estimate the SOC and capacity of each cell. With successful implementation of this scheme, cell balancing, charge/discharge control, and SOH prediction can be more accurately achieved. In particular, the capacity estimation allows the BMS to control the cell-charging rate to be proportional to its capacity so that cell imbalance during charge/discharge can be minimized. Then, the SOC estimation provides the target reference values to reach cell balance.

The remainder of the paper is organized into several sections. Section II describes the battery models that are used in developing cell voltage/current estimation by using only the string terminal voltage/current data. Although the methodologies of this paper can be used in different model structures, their actual derivations rely on model details. In this paper, we have selected two typical model structures. One is the basic linear circuit model, and the other is a popular nonlinear model embedded in the SimPower Systems Toolbox in Matlab/Simulink [22]. Both model structures have been validated by experimental data and used in many applications [19]–[21]. The main methodology for cell-level voltage/current estimation is presented in Section II on linear circuit models first, which shows how to apply active control of balancing circuits to derive cell voltage/current values from the string terminal voltage/current data. Since balancing circuits are necessary for Li-ion battery operation, our methodology does not carry additional hardware costs. Further issues on noisy measurement data and unknown model parameters are discussed. Extension of the methodology to nonlinear battery models is considered in Section III. Section IV is devoted to integrated SOC estimation and model parameter estimation. Estimation algorithms, recursive schemes, and convergence properties are discussed. Finally, Section V summarizes possible applications of our methodologies in some essential BMS functions.

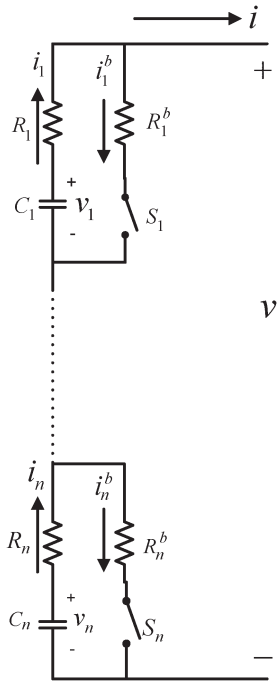

Fig. 1. Battery cell string with shunt resistor balancing circuits.

II. Control of Balancing Circuits for Enhanced Observability on Battery Systems

To facilitate discussions on the key issues and challenges in real-time battery model identification and state estimation, we first employ, as a typical simplified model structure, the resistance–capacitance battery model, which is part of ADVISOR which was developed at National Renewable Energy Laboratory [19], [20].

A battery pack contains battery cells in serial and parallel connections. At present, for safety and battery management, cell-level measurements are common, including cell terminal voltage and cell thermal sensors. In this section, we specify the battery model structures that will be used subsequently for development of adaptive management strategies. It is noted that balancing circuits create a set of possible battery circuit configurations. Consequently, balancing circuit switching can be represented by a hybrid system, whose switching index α takes values in a finite set of possible circuit configurations.

A battery string with a typical passive balancing circuit is shown in Fig. 1. The primary purpose of the passive balancing circuit is to adjust charge/discharge rates for each battery cell. For a comparison of different cell-balancing circuits, we refer the reader to [11]. The ON-state resistors of the balancing circuit are design variables, which can be selected according to the required speed of balancing, power consumption, thermal management, etc. Control of the on–off switching can be used in a pulse-width modulation (PWM) fashion to further adjust balancing rates. In this paper, we use the existing balancing circuit by controlling it to enhance system observability. The main idea is to switch the shunt for a very small time interval to temporally create a partially observable subsystem. Since the duration of such a switch is very small in comparison with the charge/discharge time, this operation has negligible effect on normal cell-balancing operations.

A. Cell Voltage Computation for Linear Circuit Models of Battery Systems Under Passive Balancing Circuits

In Fig. 1, when a balancing shunting circuit switches at t from "off" to "on," we use time t_- to denote the time right before switching and t_+ to denote the time right after switching. i is the string current (in amperes); v is the string terminal voltage (in volts); v_i is the cell open-circuit voltage, which is the capacitor voltage in the model; and R_i is the ith cell's internal resistance. The balancing shunt resistance is R_i^b. The positive directions of voltages and currents are defined as marked in Fig. 1.

We shall consider a string of n cells. To describe the basic ideas, we will use the switching of the first cell as a representative example. Denote $\widetilde{v} = v_2 + \cdots + v_n$ and $\widetilde{R} = R_2 + \cdots + R_n$. $v_- = v(t_-)$ and $i_- = i(t_-)$ are the values of v and i, respectively, at t_-; and v_+ and i_+ are the values of v and i, respectively, at t_+; and similarly, $i_{1+} = i_1(t_+)$, etc. Assume that only the string terminal v and i are measured. Neither the cell terminal voltage nor cell branch current i_1 or i_1^b are measured.

For now, we assume that all model parameters are known. Suppose that, at t_-, all balancing switches are in "off" positions. In this case, $i_{1-} = \cdots = i_{n-} = i_-$. The string terminal voltage is

$$v_- = v_1 + \widetilde{v} - (R_1 + \widetilde{R})i_-. \tag{1}$$

At t_+, switch S_1 is turned "on," but all other switches remain in "off" positions. The corresponding string terminal voltage becomes

$$v_+ = v_1 + \widetilde{v} - R_1 i_{1+} - \widetilde{R} i_+ \tag{2}$$

where the cell open-circuit voltages remain same due to capacitance.

From

$$v_1 - R_1 i_{1+} = R_1^b i_{1+}^b, \quad i_+ + i_{1+}^b = i_{1+}$$

we have

$$v_1 - R_1 i_{1+} = R_1^b(i_{1+} - i_+) = R_1^b i_{1+} - R_1^b i_+.$$

This implies

$$i_{1+} = \frac{1}{R_1 + R_1^b}\left(v_1 + R_1^b i_+\right). \tag{3}$$

It follows that

$$\begin{aligned} v_+ &= v_1 + \widetilde{v} - \frac{R_1}{R_1 + R_1^b}\left(v_1 + R_1^b i_+\right) - \widetilde{R} i_+ \\ &= \frac{R_1^b}{R_1 + R_1^b} v_1 + \widetilde{v} - \left(\frac{R_1 R_1^b}{R_1 + R_1^b} + \widetilde{R}\right) i_+. \end{aligned}$$

Consequently, the net change in the terminal voltage before and after the switching of S_1 is

$$\begin{aligned} \delta_1 &= v_+ - v_- \\ &= -\frac{R_1}{R_1 + R_1^b} v_1 - \left(\frac{R_1 R_1^b}{R_1 + R_1^b} + \widetilde{R}\right) i_+ + (R_1 + \widetilde{R}) i_-. \end{aligned}$$

Since δ_1, i_-, and i_+ are all measured, v_1 can be calculated.

In the common case $i_+ = i_- = i$ (constant current load), this expression is simplified to

$$\delta_1 = -\frac{R_1}{R_1 + R_1^b} v_1 + \frac{(R_1)^2}{R_1 + R_1^b} i. \tag{4}$$

B. Noise Attenuation

The aforementioned algorithms for estimating cell internal voltages from the string terminal voltage are accurate under noise-free voltage measurements. However, estimation accuracy is quite sensitive to measurement noises. To attenuate noise impact on estimates, we introduce the following averaging method:

Suppose that, at a selected time t, $v_1(t)$ of the first cell is to be estimated. For a small time interval of length t_0, we apply fast switching of S_1 $2N_0$ times in $[t, t + t_0]$ and calculate N_0 voltage jumps $\delta_1(k), k = 1, \ldots, N_0$. Then, the average of the jumps is calculated as

$$\bar{\delta}_1 = \frac{1}{N_0} \sum_{k=1}^{N_0} \delta_1(k).$$

$\bar{\delta}_1$ is then used in place of δ_1 in the aforementioned algorithms.

The theoretical foundation is that, if the measurement noise is independent and identically distributed with zero mean and variance σ^2, then by this averaging, the error on $\bar{\delta}_1$ is also of zero mean but with a much-reduced variance of σ^2/N_0. Consequently, much more accurate voltage estimates can be achieved.

C. Unknown Parameters and Joint Estimation Problems

In practice, the model parameters C_j and R_j for the jth cell are unknown *a priori* and change with operating conditions and cell aging. Consequently, for real-time usage in BMS, each cell's model parameters need to be estimated jointly with the OCV v_j.

Assume that the load current i is smooth (so that $i(t_+) = i(t_-) = i(t)$). For discussion, we use $j = 1$ as a generic cell. Suppose that S_1 has been switched on m times, starting at t_k with duration τ_k, $k = 1, \ldots, m$, i.e., "on" in $[t_k, t_k + \tau_k)$ and "off" in $[t_k + \tau_k, t_{k+1})$. Based on (4)

$$\delta_1(t_k) = -\frac{R_1}{R_1 + R_1^b} v_1(t_k) + \frac{(R_1)^2}{R_1 + R_1^b} i(t_k). \tag{5}$$

Furthermore, the dynamic system for $v_1(t)$ can be derived as follows: When S_1 is turned on in $[t_k, t_k + \tau_k)$, $i_1(t)$ is determined by (3) and

$$C_1 \frac{dv_1(t)}{dt} = -i_1(t) = -\frac{1}{R_1 + R_1^b} v_1(t) - \frac{R_1^b}{R_1 + R_1^b} i(t).$$

Hence

$$v_1(t_k + \tau_k) = e^{-\frac{1}{C_1(R_1 + R_1^b)}\tau_k} v_1(t_k) + q_k^{11} \tag{6}$$

where $q_k^{11} = -(R_1^b/(C_1(R_1+R_1^b)))\int_{t_k}^{t_k+\tau_k} e^{-1/(C_1(R_1+R_1^b))(t_k+\tau_k-t)} i(t)dt$. When S_1 is turned off in $[t_k+\tau_k, t_{k+1})$, $i_1(t) = i(t)$, and $C_1(dv_1(t)/dt) = -i(t)$. Then

$$v_1(t_{k+1}) = v_1(t_k+\tau_k) + q_k^{12} \tag{7}$$

where $q_k^{12} = -1/C_1 \int_{t_k+\tau_k}^{t_{k+1}} i(t)dt$. Combining (6) and (7), we have

$$v_1(t_{k+1}) = e^{-\frac{1}{C_1(R_1+R_1^b)}\tau_k} v_1(t_k) + q_k^1$$

where $q_k^1 = q_k^{11} + q_k^{12}$ is calculated from $i(t)$ and, hence, is a known value. Iteration on k implies that

$$v_1(t_{k+1}) = e^{-\frac{1}{C_1(R_1+R_1^b)}\sum_{l=1}^{k}\tau_l} v_1(t_1) + \sum_{l=1}^{k-1} e^{-\frac{1}{C_1(R_1+R_1^b)}\sum_{p=l+1}^{k}\tau_p} q_l^1 + q_k^1.$$

This expression may be written as

$$v_1(t_{k+1}) = \widetilde{h}_{k+1}(\theta_1, v_1(t_1))$$

where $\theta_1 = [C_1, R_1, R_1^b]'$. Substituting this into (5), we have

$$\delta_1(t_k) = -\frac{R_1}{R_1+R_1^b}\widetilde{h}_k(\theta_1, v_1(t_1)) + \frac{(R_1)^2}{R_1+R_1^b} i(t_k)$$

which can be compactly expressed as

$$\delta_1(t_k) = h_k(\theta_1, v_1(t_1)) + g(\theta_1) i(t_k), \qquad k = 1, \ldots, m \tag{8}$$

where

$$h_k(\theta_1, v_1(t_1)) = -\frac{R_1}{R_1+R_1^b}\widetilde{h}_k(\theta_1, v_1(t_1))$$

$$g(\theta_1) = \frac{(R_1)^2}{R_1+R_1^b}.$$

The joint estimation problem aims to estimate θ_1 and $v_1(t_1)$ simultaneously from the m equations in (8). The algorithms for solving this joint estimation problem and their convergence properties will be presented in Section IV.

D. Illustrative Examples

Example 1—Noise-Free Observations: Suppose that the load current is kept as a constant $i = 1$ (in amperes) and the string contains only two cells (see Fig. 2), which also indicates the positive directions of voltages and currents. For analysis, we consider the three relevant circuit configurations: 1) Both switches are "off." 2) S_1 is "on," but S_2 is "off." 3) S_2 is "on," but S_1 is "off." The state space models for these configurations are summarized as follows: Let $x = [v_1, v_2]'$, where x' is the transpose of x.

1) Both S_1 and S_2 are "off," i.e.,

$$\dot{x} = \begin{bmatrix} 0 & 0 \\ 0 & 0 \end{bmatrix} x + \begin{bmatrix} -\frac{1}{C_1} \\ -\frac{1}{C_2} \end{bmatrix} i$$

$$v = [1, 1]x + (R_1 + R_2)i.$$

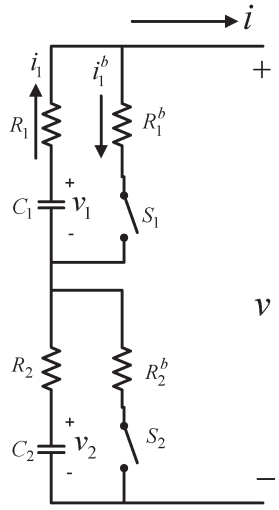

Fig. 2. Two-cell string with balancing circuits.

2) S_1 is "on," but S_2 is "off," i.e.,

$$\dot{x} = \begin{bmatrix} \frac{-1}{C_1(R_1+R_1^b)} & 0 \\ 0 & 0 \end{bmatrix} x + \begin{bmatrix} -\frac{R_1^b}{C_1(R_1+R_1^b)} \\ -\frac{1}{C_2} \end{bmatrix} i$$

$$v = \left[\frac{R_1}{R_1+R_1^b}, 1\right] x - \left(\frac{R_1 R_1^b}{R_1+R_1^b} + R_2\right) i.$$

3) S_2 is "on," but S_1 is "off," i.e.,

$$\dot{x} = \begin{bmatrix} 0 & 0 \\ 0 & \frac{-1}{C_2(R_2+R_2^b)} \end{bmatrix} x + \begin{bmatrix} -\frac{1}{C_1} \\ -\frac{R_2^b}{C_2(R_2+R_2^b)} \end{bmatrix} i$$

$$v = \left[1, \frac{R_2}{R_2+R_2^b}\right] x - \left(\frac{R_2 R_2^b}{R_2+R_2^b} + R_1\right) i.$$

Assume that the cells have the following true parameters: $C_1 = 80\,000$ F, $R_1 = 0.11$ (Ω), $R_1^b = 5$ (Ω), $C_2 = 75\,000$ F, $R_2 = 0.13$ (Ω), and $R_2^b = 5.5$ (Ω). The initial voltages on the capacitors are $v_1(0) = 3.1$ V and $v_2(0) = 3.4$ V. We start with the normal discharge operation when both S_1 and S_2 are off. The first switching occurs at $T = 60$ s when switch S_1 is turned on, but S_2 remains off. At $T = 120$, switch S_1 is turned off, and the battery system returns to normal operation. Then, at $T = 180$, switch S_2 is turned on, and S_1 remains off. The trajectories of the cell capacitor voltages and the string terminal voltage are plotted in Fig. 3.

The actual cell internal voltages and their estimates are given as follows: At $T = 60$, the actual voltage of cell 1 is $v_1(60) = 3.0993$, and its estimate is $\widehat{v}_1(60) = 3.0994$. At $T = 180$, the actual voltage of cell 2 is $v_2(60) = 3.3976$, and its calculated estimate is $\widehat{v}_2(60) = 3.3977$.

Example 2—Noisy Observations: The aforementioned cell internal voltage estimation is sensitive to measurement noises. For the same system and estimation algorithm as in Example 1, suppose that the voltage measurement is subject to noises of uniform distribution in $[-0.01, 0.01]$, representing a high-precision voltage sensor. The trajectories of the cell capacitor voltages and the string terminal voltage are plotted in Fig. 4. A sample of the estimates shows the following values: At

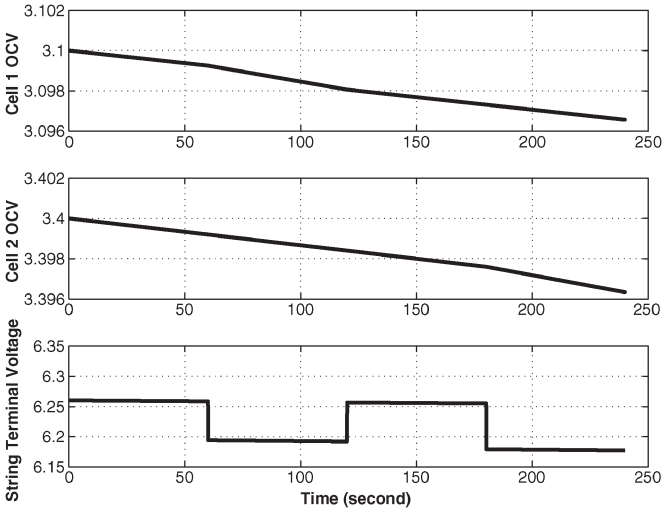

Fig. 3. Cell and terminal voltage trajectories under noise-free observations.

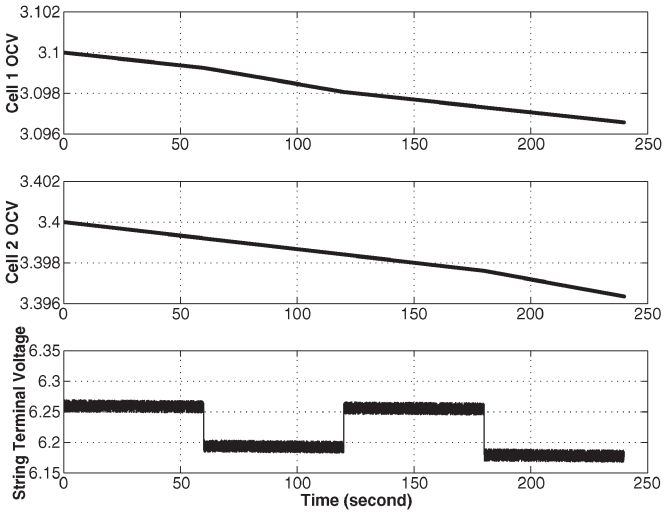

Fig. 4. Cell and terminal voltage trajectories under noisy observations on the string terminal voltage.

$T = 60$, the actual voltage of cell 1 is $v_1(60) = 3.0993$, and its calculated estimate is $\widehat{v}_1(60) = 2.8826$. At $T = 180$, the actual voltage of cell 2 is $v_2(60) = 3.3976$, and its calculated estimate is $\widehat{v}_2(60) = 2.8895$. Clearly, the accuracy is lost.

Example 3—Noisy Observations and Estimation With Averaging: To improve estimation accuracy, we now apply the fast switching scheme with estimate averaging. At the time of estimating $v_1(60)$, we apply a fast switching of 400 ($N_0 = 200$) switching in the interval of 8 s. The calculated string terminal voltage jumps are observed and then averaged. The averaged value is then used to estimate $v_1(60)$. This is repeated for the v_2 estimation at $T = 180$. Under the same noise condition as Example 2, the trajectories of the cell capacitor voltages and the string terminal voltage are plotted in Fig. 5. A sample of the estimates shows the following values: At $T = 60$, the actual voltage of cell 1 is $v_1(60) = 3.0993$, and its calculated estimate is $\widehat{v}_1(60) = 3.0965$. At $T = 180$, the actual voltage of cell 2 is $v_2(60) = 3.3976$, and its calculated estimate if $\widehat{v}_2(60) = 3.3753$. These results indicate much improved estimation accuracy.

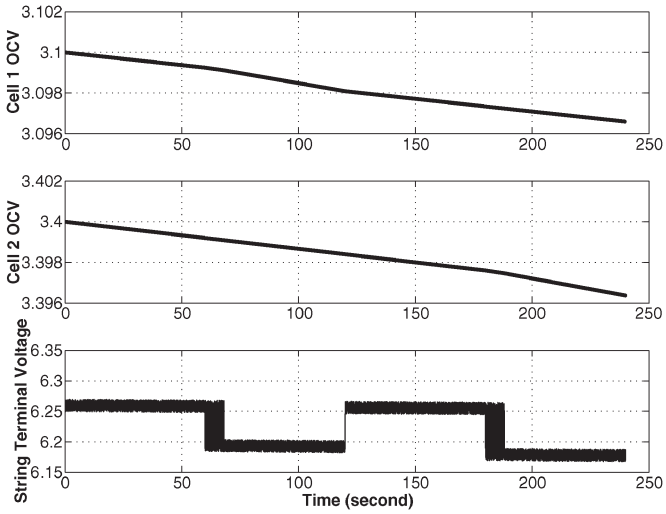

Fig. 5. Cell and terminal voltage trajectories under noisy observations and fast switching schemes.

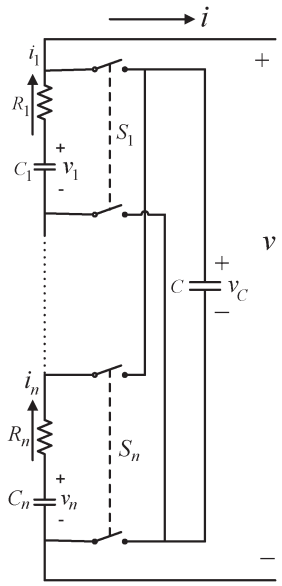

Fig. 6. Battery cell string with energy shuffling balancing circuits.

E. Algorithms for Linear Circuit Models of Battery Systems Under Energy Shuffling Balancing Circuits

The shunt resistor circuit in Fig. 1 is the simplest structure for cell balancing. When a cell's SOC is evaluated to be higher than others, its bypass circuit is turned on, and the cell is discharged to reduce its SOC. The energy is lost as heat through the shunt resistor during the balancing. As a result, this cell-balancing structure reduces battery efficiency. In contrast, the energy shuffling circuit in Fig. 6 will connect the cell with the highest SOC in the string to the balancing capacitor and charge the capacitor. The energy stored in the capacitor is then shuffled to the cell with the lowest SOC. Under this balancing structure, we assume that the string current, the string terminal voltage, and the voltage of the shuffling capacitor are measured. The cell-level voltage sensors are eliminated.

Suppose that, at time t, switch S_1 is turned to "on" position. Referring to Fig. 6, we denote $\widetilde{v}_2(t) = v_2(t) + \cdots + v_n(t)$ and

$\widetilde{R}_2 = R_2 + \cdots + R_n$. Suppose that right before t (and right after t), the terminal voltage and current are v_- and i_- (and v_+ and i_+), respectively. Since $v_c(t)$ is measured and is continuous at t, it is available in our calculation.

At t_-

$$v_- = v_1 + \widetilde{v}_2 - i_-(R_1 + \widetilde{R}_2)$$

and at t_+

$$v_+ = v_c + \widetilde{v}_2 - i_+\widetilde{R}_2.$$

Consequently, the terminal voltage difference is

$$\begin{aligned}\delta_1 &= v_+ - v_- \\ &= -v_1 + i_-(R_1 + \widetilde{R}_2) + v_c - i_+\widetilde{R}_2 \\ &= -v_1 + (i_- - i_+)\widetilde{R}_2 + i_-R_1 + v_c.\end{aligned}$$

It follows that

$$v_1 = -\delta_1 + v_c + (i_- - i_+)\widetilde{R}_2 + i_-R_1. \tag{9}$$

As a result, v_1 is estimated from measurement data on the terminal voltage, terminal current, and the shuffling capacitor voltage, eliminating the cell voltage sensors.

Although the algorithms for estimating the cell OCV under the energy shuffling balancing circuit are different from these under the shunt resistor balancing circuit, they follow the same principles. Since v_c is available, the derivations are, in fact, simpler. We note that the previous discussions on noisy observations and noise attenuation under the shunt resistor balancing circuit can also be directly applied here. Due to their similarity, these will not be repeated here.

III. State and Parameter Estimation on Nonlinear Battery Models

Although the goal of cell balancing is justifiably to equalize SOCs, for its run-time implementation, accurate SOC estimation and capacity determination are difficult. Consequently, many existing cell balancing systems are actually cell-voltage-balancing circuits. In other words, by comparing cell voltages, the balancing circuits try to equalize cell terminal voltages. This technology has fundamental drawbacks. Since terminal voltages are affected by cell impedances, which are partially the reason for cell imbalance, equalizing terminal voltages will leave SOC uneven. In other words, terminal voltage balancing is always subject to imbalance on SOCs. In addition, the characteristic curves (terminal voltage versus depth of charge/discharge) vary from cell to cell. When a cell ages, the cell voltage will be a poor indicator of its SOC. This is an acute problem for Li-ion batteries since their characteristic curves are quite flat in the normal operating ranges.

This section will present joint estimation algorithms for SOC and model parameters that only use the string terminal voltage/current measurements to achieve individual cells' SOC and parameter estimation simultaneously.

Battery monitoring, control, diagnosis, and management require parameter estimation and SOC estimation. We now show how the method described in the previous sections can be applied to this problem which is fundamental in BMS. Although the linear circuit model of the previous sections have been used in BMS, more commonly used and more accurate models are nonlinear. As a result, we will use the nonlinear circuit models embedded in the SimPower Systems Toolbox in Matlab/Simulink [21], [22] to illustrate how the aforementioned ideas can be used in nonlinear battery models.

A. Model Structures

For a string of n cells, the nonlinear circuit model for the jth cell has the output equation in the form

$$v_j = h_j - g_j i_j, \qquad j = 1, 2, \ldots, n \tag{10}$$

where v_j is the cell terminal voltage, and i_j is the cell current.[1] Functions h_j and g_j depend on the open-circuit voltage, cell capacity, SOC, polarization coefficient, etc. The equations we derive here will later be used to estimate these variables.

Based on the model from the SimPower Systems Toolbox in Matlab/Simulink [21], [22], we derived in [23] a simplified model structure for a Li-ion battery (a cell or a module). For a single cell, Liu *et al.* [23] introduced a method to jointly estimate model parameters and SOC. The situation here is more complicated due to cell-to-cell interconnections in a string.

The dynamic model for the SOC of the jth cell is

$$\dot{s}_j = -\frac{1}{Q_j}\frac{i_j}{3600}, \qquad j = 1, \ldots, n \tag{11}$$

where s_j and Q_j are the SOC and the maximum capacity of the jth cell, respectively.

To illustrate algorithm development, we have chosen the discharge operation for discussion. In addition, for simplicity, in this paper, thermal dynamics is neglected. During the discharge operation, the output function takes the form

$$v_j(t) = E_{0j} - K_j\frac{Q_j\,(1 - s_j(t))}{s_j(t)} - \left(\frac{K_j}{s_j(t)} + R_j\right) i_j(t) \tag{12}$$

which contains four unknown parameters E_{0j} (internal potential), K_j (polarization coefficient), Q_j (capacity), R_j (internal impedance), and the SOC $s_j(t)$.

Suppose that the starting time for discharge is t_0 and the SOC at t_0 is $s_j(t_0) = s_{0j}$, which is unknown. From

$$\dot{s}_j = -\frac{1}{Q_j}\frac{i_j}{3600}$$

we have

$$s_j(t) = s_{0j} - \frac{\lambda_j(t)}{Q_j}$$

[1] We emphasize that v_j is the *terminal* voltage and not the open-circuit voltage of the cell. Estimation of the open-circuit voltage, cell capacity, SOC, and model parameters will be presented later.

where

$$\lambda_j(t) = \frac{1}{3600}\int_{t_0}^{t} i_j(\tau)\,d\tau.$$

$\lambda_j(t)$ is calculated from the derived $i_j(t)$ and, hence, is known. The simplified output equation (12) becomes

$$\begin{aligned} v_j(t) &= E_{0j} - K_j\frac{Q_j\,(1-s_j(t))}{s_j(t)} - K_j\frac{i_j(t)}{s_j(t)} - R_j i_j(t) \\ &= E_{0j} + K_jQ_j - \frac{K_jQ_j}{s_{0j}-\frac{1}{Q_j}\lambda_j(t)} \\ &\quad - \left(\frac{K_j}{s_{0j}-\frac{1}{Q_j}\lambda_j(t)} + R_j\right) i_j(t) \\ &= h_j - g_j i_j(t) \end{aligned}$$

where

$$h_j = E_{0j} + K_jQ_0 - \frac{K_jQ_j}{s_{0j}-\frac{1}{Q_j}\lambda_0(t)},\ g_j = \frac{K_j}{s_{0j}-\frac{1}{Q_j}\lambda_j(t)} + R_j.$$

Under this expression, the five unknown parameters of the cell model are E_{0j}, K_j, Q_j, R_j, and the initial state-of-charge s_{0j}. For estimation of these unknown parameters, we use $\theta_j = [E_{0j}, K_j, Q_j, R_j, s_{0j}]'$, $j = 1,\ldots,n$, and $\theta = [\theta_1,\ldots,\theta_n]$. θ represents $5n$ unknown parameters to be estimated. To indicate clearly the unknown parameters, we will use

$$v_j(t) = h_j\left(\theta_j;\lambda_j(t)\right) - g_j\left(\theta_j;\lambda_j(t)\right) i_j(t). \tag{13}$$

B. Cell Terminal Voltage Estimation From String Voltage/Current Data

We now show how cell voltages can be derived from string voltage/current data. The goal is to derive the cell terminal voltage v_j. Assume that, at t_-, all switches are in "off" positions. For the first cell, its terminal voltage at t_- is

$$v_{1-} = h_1 - g_1 i_{1-}$$

and at t_+

$$v_{1+} = h_1 - g_1 i_{1+}.$$

From

$$h_1 - g_1 i_{1+} = R_1^b i_{1+}^b; \quad i_+ + i_{1+}^b = i_{1+}$$

we have

$$h_1 - g_1 i_{1+} = R_1^b(i_{1+} - i_+) = R_1^b i_{1+} - R_1^b i_+.$$

Hence

$$i_{1+} = \frac{h_1 + R_1^b i_+}{g_1 + R_1^b}.$$

It follows that

$$\begin{aligned} v_{1+} &= h_1 - \frac{g_1}{g_1+R_1^b}\left(h_1 + R_1^b i_+\right) \\ &= \frac{R_1^b}{g_1+R_1^b}h_1 - \frac{g_1R_1^b}{g_1+R_1^b}i_+. \end{aligned}$$

Now, the string terminal voltage is

$$v_- = v_{1-} + \cdots + v_{n-} = h_1 - g_1 i_- + \cdots + h_n - g_n i_-.$$

$$v_+ = \frac{R_1^b}{g_1+R_1^b}h_1 - \frac{g_1R_1^b}{g_1+R_1^b}i_+ + h_2 - g_2 i_+ + \cdots + h_n - g_n i_+.$$

Consequently, the net change in the string terminal voltage is

$$\begin{aligned} \delta_1 &= v_+ - v_- \\ &= -\frac{g_1}{g_1+R_1^b}h_1 - \frac{g_1R_1^b}{g_1+R_1^b}i_+ + g_1 i_- \\ &\quad + (g_2 + \cdots + g_n)(i_- - i_+). \end{aligned}$$

Let $\varepsilon = i_+ - i_-$ and $\widetilde{g} = g_2 + \cdots + g_n$. Then

$$\begin{aligned} \delta_1 &= -\frac{g_1}{g_1+R_1^b}h_1 - \frac{g_1R_1^b}{g_1+R_1^b}(i_- + \varepsilon) + g_1 i_- - \widetilde{g}\varepsilon \\ &= -\frac{g_1}{g_1+R_1^b}(h_1 - g_1 i_-) - \left(\frac{g_1R_1^b}{g_1+R_1^b} + \widetilde{g}\right)\varepsilon. \end{aligned}$$

Since $h_1 - g_1 i_- = v_{1-}$, we have

$$\delta_1 = -\frac{g_1}{g_1+R_1^b}v_{1-} - \left(\frac{g_1R_1^b}{g_1+R_1^b} + \widetilde{g}\right)\varepsilon. \tag{14}$$

While (14) implies that v_{1-} can be derived as

$$v_{1-} = -\frac{g_1+R_1^b}{g_1}\left(\delta_1 + \left(\frac{g_1R_1^b}{g_1+R_1^b} + \widetilde{g}\right)\varepsilon\right)$$

for parameter and SOC estimation, (14) will be used directly.

Relationships (13) and (14) lead to the following observation equation for the jth cell:

$$\begin{aligned} \delta_j &= -\frac{g_j(\theta_j;\lambda_j(t))}{g_j\left(\theta_j;\lambda_j(t)\right) + R_j^b}\left(h_j\left(\theta_j;\lambda_j(t)\right) - g_j\left(\theta_j;\lambda_j(t)\right) i_-\right) \\ &\quad - \left(\frac{g_j\left(\theta_j;\lambda_j(t)\right)R_j^b}{g_j\left(\theta_j;\lambda_j(t)\right) + R_j^b} + \sum_{l\neq j} g_l\left(\theta_l;\lambda_l(t)\right)\right)\varepsilon \\ &= f(j;\theta), \qquad j = 1,\ldots,n. \end{aligned}$$

Since all the parameters are estimated together, for algorithm development, we will suppress the cell notation j and write these observation equations in terms of the time index l:

$$\delta(l) = f_l(\theta), \qquad l = 1,2,\ldots,k \tag{15}$$

for a total of N observations. In algorithm implementation, one may simply generate equations for the cells periodically, i.e., $\delta(1)$ for cell $1,\ldots,\delta(n)$ for cell n, $\delta(n+1)$ for cell 1, etc. However, this is not mandatory.

From (15), we have a total of k equations to solve for $5n$ unknowns contained in θ. These equations may be compactly expressed as

$$\Delta_k = F_k(\theta) \tag{16}$$

where $F_k = [f_1(\theta), \ldots, f_k(\theta)]'$, and $\Delta = [\delta(1), \ldots, \delta(k)]'$. Estimation algorithms and their properties are discussed in the next section.

IV. Estimation Algorithms

Estimation algorithms aim to solve (16) for θ. Due to observation noises on v and i, the measured or calculated values of $\delta(l)$ and $f_l(\theta)$ are noise corrupted, i.e.,

$$\delta(l) = f_l(\theta) + d_l \tag{17}$$

where d_l represents the consolidated measurement noises. Thus, the actual equations will be

$$\Delta_k = F_k(\theta) + D_k \tag{18}$$

where $D_k = [d_1, \ldots, d_k]'$ is the noise vector. As a result, we are seeking approximate solutions to (18) for a finite k and convergence properties when $k \to \infty$.

The estimation algorithms developed in [23] for joint estimation of SOC and parameters are limited to individual cells. In the framework investigated in this paper, cell- to-cell interaction is a key factor to be considered. This is apparent in (16) since each equation contains parameters from all cells.

For a fixed k, due to nonlinearity, approximate solutions to (18) cannot be easily found. Then, "iterative" algorithms are used to search for more accurate solutions. Numerical implementation will designate a number L of iterations for algorithm execution. Symbol $\widehat{\theta}_k(l)$ means the estimate of θ obtained on the basis of k equations after l iterations. On the other hand, when the data size is increased from k to $k+1$, to avoid repeating of the whole search process, a "recursive" algorithm employs $\widehat{\theta}_k(L)$ as the starting point $\widehat{\theta}_{k+1}(0)$ to save computational and data storage complexity.

A. Block Data Iterative Search Algorithm

Suppose that we have a set of $k \geq 5n$ observation equations and would like to search for a solution to $\Delta_k = F_k(\theta)$. Starting from an initial estimate $\widehat{\theta}_k(0)$, the iterative search algorithm takes the form

$$\widehat{\theta}_k(l+1) = \widehat{\theta}_k(l) + \varepsilon_l G_k\left(\widehat{\theta}_k(l)\right)\left(\Delta_k - F_k\left(\widehat{\theta}_k(l)\right)\right) \tag{19}$$

for $l = 1, \ldots, L$, where

$$G_k\left(\widehat{\theta}_k(l)\right) = \left(J_k\left(\widehat{\theta}_k(l)\right)' J_k\left(\widehat{\theta}k(l)\right)\right)^{-1} J_k\left(\widehat{\theta}k(l)\right)'.$$

This is a gradient-based search with variable step sizes ε_l. For convergence, it is typical to select the step size as $\varepsilon_l = K_0/l^\rho$ for some constants $K_0 > 0$ and $1/2 < \rho \leq 1$. Selection of the step sizes is important and depends on specific problems. For a specific model structure, some tuning of the step size is important for achieving good tradeoff between convergence speed and accuracy.

Remark 1: The invertibility of $J_k(\widehat{\theta}_k(l))' J(\widehat{\theta}_k(l))$ is an input design problem in which load current i needs to be varied to be sufficiently rich so that θ can be uniquely determined from (16) under noise-free environments. Usually, the input (the load current) can be slightly perturbed with a dither signal of zero mean to enhance signal richness without affecting the discharging operation. Typically, the dither can be designed to contain a sufficient number of exciting modes or to be a random signal. See [24] for further discussions on input design and persistent excitation conditions.

At the end of this iteration process, an estimate $\widehat{\theta}_k(L)$ is obtained. However, when a new data point, i.e., a new observation equation, is obtained, Δ_k and F_k are expanded by one additional entry to become Δ_{k+1} and F_{k+1}. In principle, $\widehat{\theta}_{k+1}(L)$ must be calculated by (19) again, which is computationally intensive. Recursive algorithms aim to reduce such computational complexity by using $\widehat{\theta}_k(L)$ as the initial estimate $\widehat{\theta}_{k+1}(0)$ and employing the new equation to update the estimate to $\widehat{\theta}_{k+1}(L)$, rather than recomputing the solutions to (16). Such recursive algorithms are presented next.

B. Recursive Estimation Algorithms

For computational efficiency, the algorithm will be recursive. In this regard, each time a new equation is generated from a balancing circuit switching, one new input–output relationship is added. Then

$$\Delta_{k+1} = \begin{bmatrix} \Delta_k \\ \delta(k+1) \end{bmatrix} \quad F_{k+1}(\theta) = \begin{bmatrix} F_k(\theta) \\ f_{k+1}(\theta) \end{bmatrix}.$$

Consequently, searching algorithms for solutions of θ to (16) are, in fact, stochastic approximation (SA) algorithms [25].

The main idea stems from a simultaneous recursive updating of the Jacobian matrix from $J_k(\cdot)$ to $J_{k+1}(\cdot)$ and the estimate from $\widehat{\theta}_k$ to $\widehat{\theta}_{k+1}$ when a new observation equation becomes available. The algorithm is an embedded stochastic algorithm with two loops. The outer loop resembles a recursive least-squares estimation algorithm but modified with variable step size. Due to nonlinearity, an inner loop is added, so that, for each new observation equation, an iterative search algorithm is implemented m times with time-varying step sizes. To distinguish this from the block iteration, m is usually much smaller than L due to the fact that the initial estimate in this iteration is already a good estimate.

Let

$$\phi_k(\theta) = \frac{\partial f_k(\theta)}{\partial \theta}.$$

Typically, one selects an initial data size as k_0 and performs the block data iteration search, as described in the previous subsection, L steps to obtain the initial estimate $\widehat{\theta}_{k_0}$ and select

$P_{k_0} = (J_{k_0}(\widehat{\theta}_{k_0})' J_{k_0}(\widehat{\theta}_{k_0}))^{-1}$. Then, the following iteration/recursion algorithm is performed for $k = k_0 + 1, \ldots$:

Recursive Algorithm: We index the inner loop iteration by l and the outer loop recursion by k. The algorithm thus reads

$$\widehat{\theta}_k(l+1) = \widehat{\theta}_k(l) + \rho_k(l) G_k \left(\delta(k) - f_k\left(\widehat{\theta}_k(l)\right)\right) \qquad 1 \le l \le m,$$

$$G_{k+1} = \frac{P_k \phi_k\left(\widehat{\theta}_k(m)\right)}{1 + \phi_k'\left(\widehat{\theta}_k(m)\right) P_k \phi_k\left(\widehat{\theta}_k(m)\right)}$$

$$P_{k+1} = \left(I - G_{k+1}\phi_k'\left(\widehat{\theta}_k(m)\right)\right) P_k \tag{20}$$

where $\{\rho_k(l)\}$ is a stepsize sequence similar to that used in (19).

The essence is that there are two loops: an inner iteration loop and an outer recursive loop. For a fixed index k (data size), we carry out an SA type of updates for the parameter estimates $\widehat{\theta}_k(l)$ for m steps through the inner loop with index l. When a new observation equation is available, it is used to update the gain matrix to G_{k+1} through the outer loop. This amounts to an update on the gradient matrix. Since it is a least-squares-type recursion, P_k is also updated to P_{k+1}.

Remark 2: It is noted that, unlike (19), the iteration part of the algorithm involves only a scaler inverse and hence is much simplified in its computational complexity. The recursive part of the algorithm expresses how to go from data size $k-1$ with $\widehat{\theta}_{k-1}(m)$ to data size k with $\widehat{\theta}_k(m)$. In the linear regression models, $m = 1$, and the optimal solution in the least-squares sense can be obtained in one step. In the case of nonlinear systems, m step iteration is helpful in improving estimation accuracy. In addition, the introduction of the variable step size allows further algorithm design to enhance convergence speed.

In practice, both algorithms are needed. At the beginning, we collect a sufficient number N of equations so that the Jacobian matrix becomes full rank. Then, the "Block Data Iteration Algorithm" can be performed to obtain the first estimate. This process, rather than a wild guess on θ as the initial estimate, has been shown in many practical applications to start a reasonably accurate model before applying combined two-loop iterative/recursive algorithms. After that, each time that a new observation equation becomes available, the "Recursive Algorithm" can be implemented to obtain a new Jacobian matrix and gain matrix. Then, the inner loop of iteration starts anew. Usually, m can be much smaller than L since these iteration steps start with a good estimate and only serve to gradually improve estimate accuracy.

Remarks on Convergence Analysis: Convergence analysis of the aforementioned recursive algorithm can be conducted by the ordinary differential equation approach (see [25] for a comprehensive treatment of SA algorithms and conditions on noise and step sizes under which the algorithm is consistent). Here, we only outline the main ideas.

Seeking solutions to $\Delta_k = F_k(\theta)$ under noisy observations is a typical SA problem. Our two-loop iterative/recursive algorithm can be mathematically expressed as an SA algorithm. It is well known (see [25]) that, under suitable conditions on step size $\rho_k(l)$ and gain matrix G_k, $\widehat{\theta}_k(m) \to \theta$ as $k, m \to \infty$ with probability one (w.p.1) or in some weak sense.

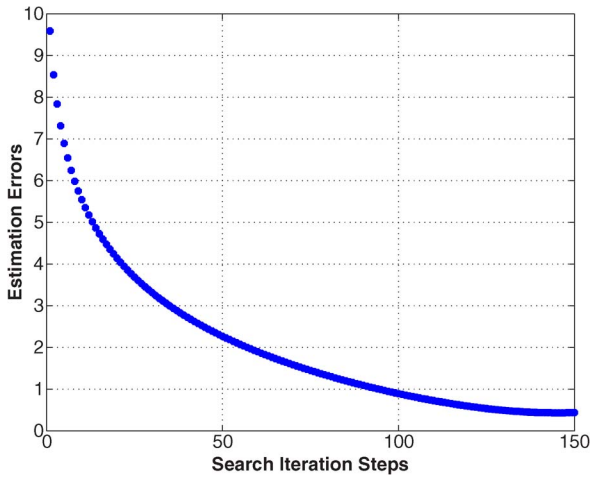

Fig. 7. Estimation error $\|\widehat{\theta}_N - \theta\|$ (Euclidian norm) as a function of the iteration step N for Example 4.

TABLE I
JOINT PARAMETER AND SOC ESTIMATION

	R	K	E_0	Q	SOC
True	0.3077	0.1737	216.6753	6.5	0.8
Estimates	0.3045	0.1639	216.7441	6.0662	0.8121

To choose appropriately gain matrix G_k to reduce the error variance, the main conclusions from [26] indicate that one may locally linearize F_k near the true parameter θ to obtain its Jacobian matrix $J_k(\theta)$. Then, by choosing the gain matrix as the solution to a corresponding Lyapunov equation, convergence of the estimates can be established. Our selection of the gain matrix is, in fact, based on the Jacobian matrix and a stable solution to the corresponding Lyapunov equation. Recursifying the gain matrix calculation leads to our outer loop algorithm. In practical implementation, the true θ is unknown. Commonly, θ is then replaced by its estimate $\widehat{\theta}_k(m)$ in algorithms. This is also the case with our algorithm. In addition, the idea of iterate averaging (see [25, Chap. 11], [28], [29], and references therein) can be used to further improve estimate accuracy. Due to scope limitations, this additional algorithm is not included in this paper. For further information on SA algorithm development and essential convergence properties, one may consult [25]–[29]. Different modes of convergence of probability measures can be found in [30].

C. Simulation Examples on Joint Estimation of Parameters and OCVs

Example 4: We shall use a demo battery system in SimPower Toolbox of Matlab/Simulink as a benchmark example to illustrate how to use voltage/current data for a battery module to estimate jointly battery model parameters and SOC. The battery model parameters are $R = 0.3077$, $K = 0.1737$, $E_0 = 216.6753$, and $Q = 6.5$. The initial SOC is 0.8. Fig. 7 shows how the estimation error is reduced with estimation iterative steps. The exit values of the estimated parameters and SOC are compared with the true values in Table I.

V. Conclusion

This paper has presented a novel methodology that derives cell voltage/current estimation from the string terminal voltage/current data and combines SOC and cell parameter estimation. This methodology can be used to enhance BMS. First, accurate cell SOC estimation will allow more accurate cell-balancing operation. This will overcome the key drawback of balancing cell terminal voltages, which are inadequate as indicators of SOC, particularly for Li-ion batteries. Second, SOC estimation is the key for charge/discharge control. Furthermore, estimation of cell model parameters provides some critical characteristics for SOH prediction and fault diagnosis. For example, the capacity estimate is essential for SOH prediction. Changes in capacity and internal impedance are essential variables for battery diagnosis. Our methods can form a foundation for battery diagnostic functions.

There are some issues that are related to the practical implementation of our methodologies, which need further investigation. First, for more accurate estimation, large balancing current is desirable. This, however, will increase balancing circuit power rating and energy loss. A design tradeoff needs to be evaluated to achieve a good compromise. Second, our methods should be evaluated experimentally on real batteries.

References

[1] D. Linden and T. Reddy, *Handbook of Batteries*, 3rd ed. New York: McGraw-Hill, 2001.

[2] G. Plett, "Extended Kalman filtering for battery management systems of LiPB-based HEV battery packs. Part 1. Background," *J. Power Sources*, vol. 134, no. 2, pp. 252–261, 2004.

[3] S. Rodrigues, N. Munichandraiah, and A. Shukla, "A review of state-of-charge indication of batteries by means of ac impedance measurements," *J. Power Sources*, vol. 87, no. 1/2, pp. 12–20, 2000.

[4] M. Sitterly and L. Y. Wang, "Identification of battery models for enhanced battery management," in *Proc. Clean Technol. Conf. Expo*, Anaheim, CA, Jun. 21–24, 2010.

[5] M. Sitterly, L. Y. Wang, and G. Yin, "Enhanced identification algorithms for battery models under noisy measurements," in *Proc. SAE Power Syst. Conf.*, Forth Worth, TX, Nov. 2–4, 2010.

[6] M. Sitterly, L. Y. Wang, G. Yin, and C. Wang, "Enhanced identification of battery models for real-time battery management," *IEEE Trans. Sustainable Energy*, vol. 2, no. 3, pp. 300–308, Jul. 2011.

[7] E. Barsoukov, J. Kim, C. Yoon, and H. Lee, "Universal battery parameterization to yield a nonlinear equivalent circuit valid for battery simulation at arbitrary load," *J. Power Sources*, vol. 83, no. 1/2, pp. 61–70, Oct. 1999.

[8] H. Chan and D. Sutanto, "A new battery model for use with battery energy storage systems and electric vehicle power systems," in *Proc. IEEE Power Eng. Soc. Winter Meeting*, Singapore, Jan. 23–27, 2000, pp. 470–475.

[9] L. Y. Wang, G. Yin, J.-F. Zhang, and Y. Zhao, *System Identification With Quantized Observations*. Boston, MA: Birkhäuser, 2010.

[10] K. Takano, K. Nozaki, Y. Saito, A. Negishi, K. Kato, and Y. Yamaguchi, "Simulation study of electrical dynamic characteristics of lithium-ion battery," *J. Power Sources*, vol. 90, no. 2, pp. 214–223, Oct. 2000.

[11] S. W. Moore and P. Schneider, "A review of cell equalization methods for lithium ion and lithium polymer battery systems," presented at the SAE World Congr., Detroit, MI, 2001, Paper 2001-01-0959.

[12] N. H. Kutkut, H. L. N. Wiegman, D. M. Divan, and D. W. Novotny, "Design considerations for charge equalization of an electric vehicle battery system," *IEEE Trans. Ind. Appl.*, vol. 35, no. 1, pp. 28–35, Feb. 1999.

[13] M. Chen and G. A. RinconMora, "Accurate electrical battery model capable of predicting runtime and I-V performance," *IEEE Trans. Energy Convers.*, vol. 21, no. 2, pp. 504–511, Jun. 2006.

[14] M. Dubarry, N. Vuillaume, and B. Y. Liaw, "From single cell model to battery pack simulation for Li-ion batteries," *J. Power Sources*, vol. 186, no. 2, pp. 500–507, Jan. 2009.

[15] D. W. Dennis, V. S. Battaglia, and A. Belanger, "Electrochemical modeling of lithium poly-mer batteries," *J. Power Sources*, vol. 110, no. 2, pp. 310–320, Aug. 2002.

[16] P. M. Gomadam, J. W. Weidner, R. A. Dougal, and R. E. White, "Mathematical modeling of lithium-ion and nickel battery systems," *J. Power Sources*, vol. 110, no. 2, pp. 267–284, Aug. 2002.

[17] J. Newman, K. E. Thomas, H. Hafezi, and D. R. Wheeler, "Modeling of lithium-ion batteries," *J. Power Sources*, vol. 119–121, pp. 838–843, Jun. 2003.

[18] L. Song and J. W. Evans, "Electrochemical-thermal model of lithium polymer batteries," *J. Electrochem. Soc.*, vol. 147, no. 6, pp. 2086–2095, 2000.

[19] V. Johnson, M. Zolot, and A. Pesaran, "Development and validation of a temperature-dependent resistance/capacitance battery model for ADVISOR," in *Proc. 18th Elect. Veh. Symp.*, Berlin, Germany, Oct. 2001.

[20] V. H. Johnson, "Battery performance models In ADVISOR," *J. Power Sources*, vol. 110, no. 2, pp. 321–329, Aug. 2002.

[21] O. Tremblay and L. A. Dessaint, "Experimental validation of a battery dynamic model for EV applications," in *Proc. EVS24*, vol. 3, *World Electric Vehicle Journal*, Stavanger, Norway, May 13–16, 2009.

[22] [Online]. Available: http://www.mathworks.com/help/toolbox/physmod/powersys/ref/battery.html

[23] L. Liu, L. Y. Wang, Z. Chen, C. Wang, F. Lin, and H. Wang, "Integrated system identification and state-of-charge estimation of battery systems," *IEEE Trans. Energy Convers.*, submitted.

[24] L. Ljung, *System Identification: Theory for the User*. Englewood Cliffs, NJ: Prentice-Hall, 1987.

[25] H. J. Kushner and G. Yin, *Stochastic Approximation and Recursive Algorithms and Applications*, 2nd ed. New York: Springer-Verlag, 2003.

[26] K. L. Chung, "On a stochastic approximation method," *Ann. Math. Statist.*, vol. 25, no. 3, pp. 463–483, Sep. 1954.

[27] C. Z. Wei, "Multivariate adaptive stochastic approximation," *Ann. Statist.*, vol. 15, no. 3, pp. 1115–1130, Sep. 1987.

[28] D. Ruppert, "Stochastic approximation," in *Handbook in Sequential Analysis*, B. K. Ghosh and P. K. Sen, Eds. New York: Marcel Dekker, 1991, pp. 503–529.

[29] B. T. Polyak, "New method of stochastic approximation type," *Autom. Remote Control*, vol. 7, pp. 937–946, 1991.

[30] W. Feller, *An Introduction to Probability Theory and its Applications*, 3rd ed. New York: Wiley, 1968.

Le Yi Wang (F'12) received the Ph.D. degree in electrical engineering from McGill University, Montreal, QC, Canada, in 1990.

Since 1990, he has been with Wayne State University, Detroit, MI, where he is currently a Professor in the Department of Electrical and Computer Engineering. He is currently an Associate Editor of the *Journal of System Sciences and Complexity* and the *Journal of Control Theory and Applications*. He has been a keynote speaker at several international conferences. His research interests are complexity and information, system identification, robust control, H^∞ optimization, time-varying systems, adaptive systems, hybrid and nonlinear systems, information processing and learning, as well as medical, automotive, communications, power systems, and computer applications of control methodologies.

Dr. Wang was an Associate Editor of the IEEE Transactions on Automatic Control and several other journals.

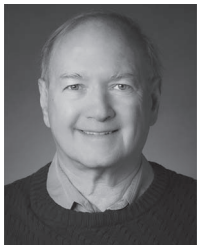

Michael P. Polis (LSM'09) received the B.S.E.E. degree from the University of Florida, Gainesville, in 1966 and the M.S.E.E. and Ph.D. degrees from Purdue, University, West Lafayette, IN, in 1968 and 1972, respectively.

From 1972 to 1983, he was a faculty member in electrical engineering with Ecole Polytechnique de Montreal, Montreal, QC, Canada. From 1983 to 1987, he directed the Systems Theory and Operations Research Program at the National Science Foundation. In 1987, he joined Wayne State University, Detroit, MI, as Chair of Electrical and Computer Engineering. From 1993 to 2001 he was the Dean of the School of Engineering and Computer Science, Oakland University, Rochester, MI, where he is currently with the Department of Industrial and Systems Engineering. He has been a consultant for several companies and an expert witness for numerous law firms. His research interests are energy systems optimization, transportation systems, and identification and control of distributed parameter systems.

Dr. Polis was a corecipient of the Best Paper Award of the IEEE TRANSACTIONS ON AUTOMATIC CONTROL (1974–1975).

G. George Yin (F'02) received the B.S. degree in mathematics from the University of Delaware, Newark, in 1983 and the M.S. degree in electrical engineering and the Ph.D. degree in applied mathematics from Brown University, Providence, RI, in 1987.

He then joined the Department of Mathematics, Wayne State University, Detroit, MI, and became a Professor in 1996. He is an Associate Editor for *SIAM Journal on Control and Optimization*, the *Journal of Control Theory and Applications*, and *Automatica* and serves on the Editorial Board of a number of other journals. His research interests include stochastic systems theory and applications.

Dr. Yin has served on many IEEE and International Federation of Automatic Control technical committees, i.e., he was a Co-Chair of the 1996 and 2003 American Mathematical Society and the Society for Industrial and Applied Mathematics (AMS-SIAM) and AMS-IMS-SIAM Summer Conferences and the 2011 SIAM Control Conference. He served as the Program Director and Vice Chair of the SIAM Activity Group on Control and Systems Theory, Chair of the SIAM Journal on Control and Optimization Best Paper Prize Committee, and member of the SIAM W. T. and Idalia Reid Prize Selection Committee. He also served as an Associate Editor for the IEEE TRANSACTIONS ON AUTOMATIC CONTROL. He is the President of Wayne State University's Academy of Scholars.

Wen Chen (M'09) received the Ph.D. degree from Simon Fraser University, Burnaby, BC, Canada, in 2004.

From 2005 to 2007, he was a Postdoctoral Researcher with the University of Louisiana, Lafayette. After that period, he worked in industrial companies as a Control Systems Engineer. He joined the Division of Engineering Technology, Wayne State University, Detroit, MI, in 2009. His teaching and research interests are control systems, alternative energy storage, and fault diagnosis of industrial systems.

Yuhong Fu received the M.S. degree in automotive systems engineering from The University of Michigan-Dearborn, in December 2011.

She is currently with the Department of Electrical and Computer Engineering, University of Michigan-Dearborn. Her research interests are battery modeling and management for electric drive vehicle applications.

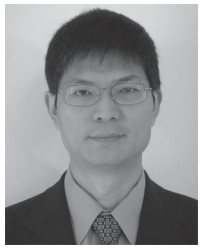

Chunting Chris Mi (S'00–A'01–M'01–SM'03–F'12) received the B.S.E.E. and M.S.E.E. degrees from Northwestern Polytechnical University, Xi'an, China, and the Ph.D. degree from the University of Toronto, Toronto, ON, Canada, all in electrical engineering.

He is currently a Professor of electrical and computer engineering and the Director of the newly established Department of Energy-funded GATE Center for Electric Drive Transportation at the University of Michigan-Dearborn. Previously, he was an Electrical Engineer with General Electric Canada, Inc. He has been a Guest Editor for the *International Journal of Power Electronics* and Associate Editor for the *Journal of Circuits, Systems, and Computers* (2007–2009) and serves on the Editorial Board of the *International Journal of Electric and Hybrid Vehicles* and *IET Electrical Systems in Transportation*. He has conducted extensive research and published more than 100 articles. His research interests include electric drives, power electronics, electric machines, renewable-energy systems, and electrical and hybrid vehicles.

Dr. Mi was the Chair (2008–2009) and Vice Chair (2006–2007) of the IEEE Southeastern Michigan Section and the General Chair of the Fifth IEEE Vehicle Power and Propulsion Conference held in Dearborn on September 6–11, 2009. He has been an Associate Editor for the IEEE TRANSACTIONS ON VEHICULAR TECHNOLOGY, the IEEE TRANSACTIONS ON POWER ELECTRONICS LETTERS, and the IEEE TRANSACTIONS ON INDUSTRY APPLICATIONS, and a Senior Editor for the IEEE VEHICULAR TECHNOLOGY MAGAZINE. He received the "Distinguished Teaching Award" and "Distinguished Research Award" from the University of Michigan-Dearborn, the 2007 IEEE Region 4 "Outstanding Engineer Award," the "IEEE Southeastern Michigan Section Outstanding Professional Award," and the "SAE Environmental Excellence in Transportation Award."